Current Biology, Vol. 13, 784–789, April 29, 2003, ©2003 Elsevier Science Ltd. All rights reserved. DOI 10.1016/S0960-9822(03)00281-1

Negative Feedback Regulation of *Dicer-Like1* in *Arabidopsis* by microRNA-Guided mRNA Degradation

Zhixin Xie, Kristin D. Kasschau, and James C. Carrington*
Center for Gene Research and Biotechnology and Department of Botany and Plant Pathology
Oregon State University
Corvallis, Oregon 97331

Summary

Formation of microRNA (miRNA) requires an RNaseIII domain-containing protein, termed DICER-1 in animals and DICER-LIKE1 (DCL1) in plants, to catalyze processing of an RNA precursor with a fold-back structure [1]. Loss-of-function *dcl1* mutants of *Arabidopsis* have low levels of miRNA and exhibit a range of developmental phenotypes in vegetative, reproductive, and embryonic tissues [2]. In this paper, we show that *DCL1* mRNA occurs in multiple forms, including truncated molecules that result from aberrant pre-mRNA processing. Both full-length and truncated forms accumulated to relatively low levels in plants containing a functional *DCL1* gene. However, in *dcl1* mutant plants, *dcl1* RNA forms accumulated to levels several-fold higher than those in *DCL1* plants. Elevated levels of *DCL1* RNAs were also detected in miRNA-defective *hen1* mutant plants and in plants expressing a virus-encoded suppressor of RNA silencing (P1/HC-Pro), which inhibits miRNA-guided degradation of target mRNAs. A miRNA (miR162) target sequence was predicted near the middle of *DCL1* mRNA, and a *DCL1*-derived RNA with the properties of a miR162-guided cleavage product was identified and mapped. These results indicate that *DCL1* mRNA is subject to negative feedback regulation through the activity of a miRNA.

Results and Discussion

Aberrant Splicing Results in Multiple *DCL1*-Derived RNAs

DICER-1 and DCL1 in animals and plants, respectively, are multidomain proteins that catalyze the formation of miRNAs [1, 2]. These RNaseIII-like proteins recognize and process precursor RNAs that adopt a self-complementary fold-back structure. Animal DICER-1, but not *Arabidopsis* DCL1, is also required for short interfering RNA (siRNA) biosynthesis from dsRNA substrates during RNA silencing or RNA interference [3, 4]. In general, miRNAs function as negative regulatory molecules during development [5]. Mature miRNAs of ~21 nucleotides in length serve as guide sequences after assembly into ribonucleoprotein complexes, such as the RNA-induced silencing complex (RISC) [6–8]. These complexes interact with mRNA targets to direct cleavage/degradation [7, 9] or to suppress translation [10, 11]. In plants, target mRNAs encoding members of several transcription factor families were predicted and validated [7, 9, 12, 13].

The *DCL1* gene (At1g01040) in *Arabidopsis* contains 20 exons and encodes a protein with 6 recognizable domains, including one helicase, one PAZ, two RNaseIII, and two dsRNA binding domains (Figure 1A) [2]. Blot hybridization assays with total or poly(A)$^+$ RNA were done by using helicase domain- or RNaseIII domain-specific probes. Full-length *DCL1* mRNA was detected in each sample (Figure 1B). However, two shorter RNAs that migrated at positions corresponding to 4.0 kb and 2.5 kb were consistently detected by using the 5′ proximal helicase domain probe and the 3′ proximal RNaseIII domain probe, respectively. The full-length and 2.5 kb RNAs, but not the 4.0 kb RNA, were detected in the poly(A)$^+$-enriched fraction (Figure 1B). A series of RNase protection assays (RPAs) and additional blot analyses revealed that the two RNAs were nonoverlapping and that the 3′ end of the 4.0 kb RNA and the 5′ end of the 2.5 kb RNA arose from sequences near the PAZ domain coding region (Figure 1B and data not shown). These data are consistent with *DCL1* hybridization and RNA accumulation patterns characterized previously [14].

Precise mapping of the ends of the *DCL1*-derived RNAs was done by using RNA ligase-mediated 3′ RACE and 5′ RACE [15]. In preliminary experiments, the 5′ end of both full-length *DCL1* mRNA and 4.0 kb RNA required 5′ decapping reactions prior to ligation with adaptor RNA; this finding suggests that both contain a 5′ cap structure. The 3′ end of 4.0 kb RNA and the 5′ end of the 2.5 kb RNA did not require any treatment prior to adaptor ligation. The 3′ RACE reactions corresponding to the 4.0 kb RNA yielded a homogeneous PCR product (Figure 1C, lane 1). Nine of ten clones from this product contained a 3′ end that mapped precisely to the exon 14/exon 15 boundary and lacked a poly(A) sequence (Figure 1C). The 5′ RACE reactions corresponding to the end of the 2.5 kb RNA yielded two populations of product (Figure 1C, lane 2). One population corresponded to RNA with a 5′ end within intron 14 (8/8 clones), and the other corresponded to RNA with a 5′ end within either exon 15 or exon 16 (10/10 clones; Figure 1C). These results suggest that the 4.0 and 2.5 kb RNAs arise from a DCL1 mRNA precursor through defective or incomplete splicing around intron 14.

To test whether or not the 4.0 and 2.5 kb *DCL1*-derived RNAs result from aberrant splicing around intron 14, two constructs were expressed and analyzed in *Nicotiana benthamiana* leaves after delivery by *Agrobacterium tumefaciens* (Agro) injection [16]. One construct (*35S:AtDCL1*) contained a full-length, intronless cDNA corresponding to the *DCL1* mRNA. The other construct (*35S:AtDCL1+in14*) contained the same cDNA, except that intron 14 was included between exon 14 and exon 15 just as it occurs within genomic DNA. Both constructs contained 35S promoter and terminator sequences. Expression of *35S:AtDCL1* resulted in accumulation of full-length mRNA, which was detected by using an RNaseIII domain probe, but no discrete 2.5 kb RNA (Figure 2B, lanes

*Correspondence: carrington@orst.edu

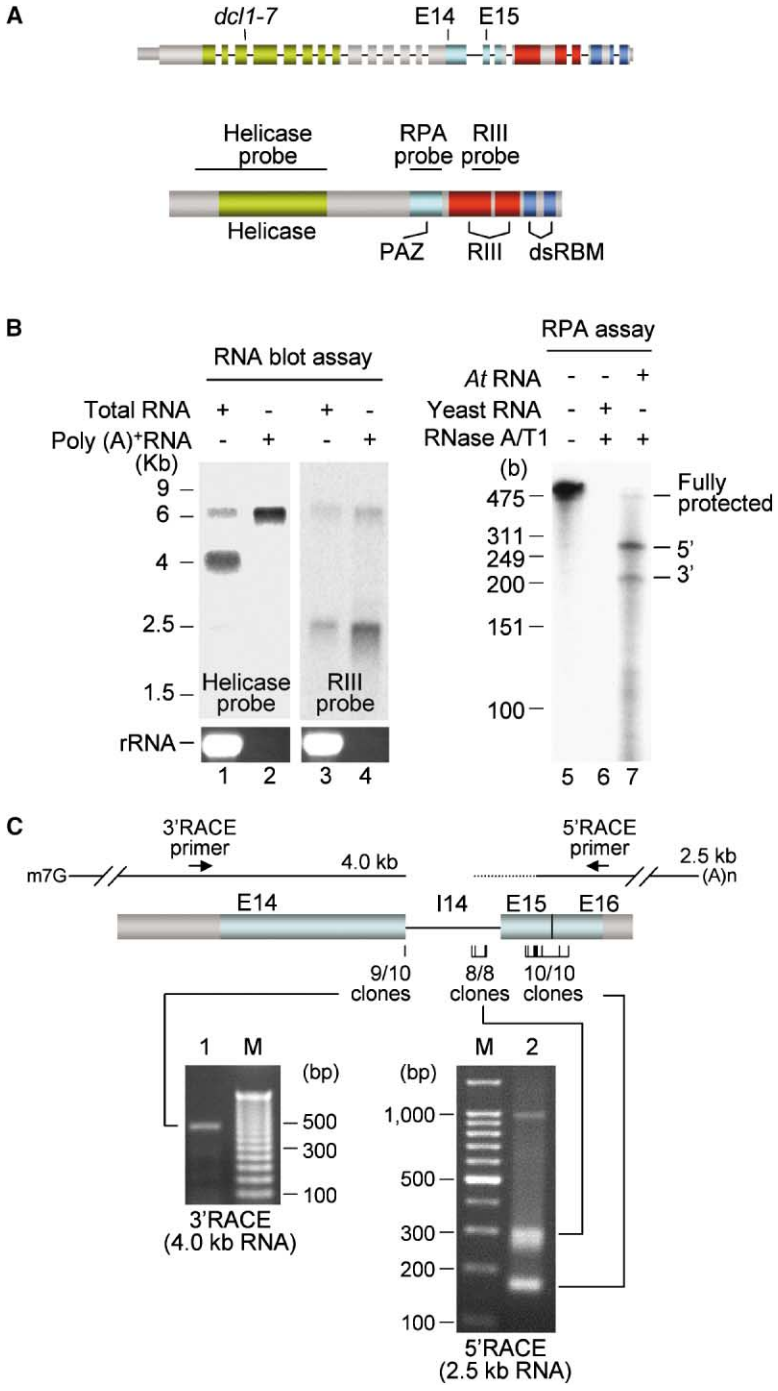

Figure 1. Detection and Analysis of *DCL1* RNA Species

(A) *DCL1* genomic DNA (upper diagram) and mRNA (lower diagram) organization. Regions that encode conserved domains in the Dicer family are indicated by colors. Locations of the cDNA-derived probe sequences are indicated by thin lines above the mRNA diagram. *dcl1-7*, *dicer like1-7* mutation; E14, exon 14; E15, exon 15; RPA, ribonuclease protection assay; RIII, RNase III; PAZ, Piwi/ARGONAUT/Zwille domain; dsRBM, dsRNA binding motif.

(B) Three species of *DCL1* RNAs revealed by the RNA blot assay and the ribonuclease protection assay (RPA). Blot hybridization of total RNA (25 μg, lanes 1 and 3) and poly(A)$^+$-enriched RNA (0.5 μg, lanes 2 and 4) samples prepared from shoot tissue of 4-week-old flowering plants (Col-0) was done by using radiolabeled probes corresponding to DCL1 helicase (nucleotides 466–2274) and RNase III (nucleotides 4336–4806) domain coding sequences. For RPA, a radiolabeled 475 nucleotide (3519–3993) RNA probe was prepared by in vitro transcription (MAXIscript T7 kit, Ambion) and was gel purified. The RPA assay reactions (RPAIII kit, Ambion) contained 50 μg *Arabidopsis* total RNA (lane 7) or control yeast RNA (lane 6), and products were resolved on a 5% denaturing polyacrylamide gel. End-labeled ϕX174/*Hin*fI DNA Markers (Promega) were used as size markers.

(C) Mapping of the 2.5 kb and 4.0 kb *DCL1* RNAs by RNA ligase-mediated RACE. An expanded diagram of the *DCL1* mRNA sequence corresponding to exon 14 (E14), exon 15 (E15), and exon 16, as well as intron 14 (I14), is shown with the same domain color scheme shown in (A). For mapping the 3′ end of the 4.0 kb RNA, *Arabidopsis* total RNA was directly ligated to an RNA adaptor (5′-CAGU AGUCGUCAAGAGUGGA-idT-3′, Dharmacon Research) and was reverse transcribed as previously described [15]. This was followed by 3′ RACE PCR with an adaptor sequence-specific reverse primer (5′-TTTTCTGCAGTC CACTCTTGACGAC-3′) and a gene-specific forward primer *DCL1*-3343F (5′-GCGTGGGA CAACCCTCTTCAGAGA-3′). The 5′ ends of the 2.5 kb RNA population were mapped by 5′ RACE as previously described [9]. The gene-specific 5′ RACE primer was *DCL1*-3993R (5′-GGGTAACCTCTGAGCACCTCGGATAAGT-3′). Ethidium bromide-stained gels showing the 3′ RACE (lane 1) and 5′ RACE (lane 2) products and size markers (M) are shown. The RACE products were cloned and sequenced. The numbers of clones containing the indicated end positions/total clones sequenced for each set of RACE products are indicated below the exon/intron diagram. The inferred positions of the ends of the 2.5 kb and 4.0 kb RNAs are shown above the exon/intron map.

4 and 9). In contrast, expression of *35S:AtDCL1+in14* yielded both full-length and 2.5 kb RNAs, each of which was detected by using RNaseIII domain and intron 14 probes (Figure 2B, lanes 5 and 10). Using total and poly(A)$^+$ RNA from *Arabidopsis* as a control, the authentic 2.5 kb RNA was detected by using the RNaseIII domain and intron 14 probes (Figure 2B, lanes 1, 2, 6, and 7), although the hybridization signals were far weaker than those corresponding to the Agro injection extracts. It was concluded, therefore, that formation of the 4.0 and 2.5 kb RNAs was dependent on intron 14.

These data indicate that the short, *DCL1*-derived RNAs arise by aberrant or incomplete splicing around intron 14. The 4.0 kb and 2.5 kb RNAs likely originate from accurate pre-mRNA cleavage at the exon 14/intron 14 boundary by the splicing apparatus, but without subsequent joining of exon 14 to exon 15. The 4.0 kb RNA maintains a relatively stable 3′ end, as indicated by the

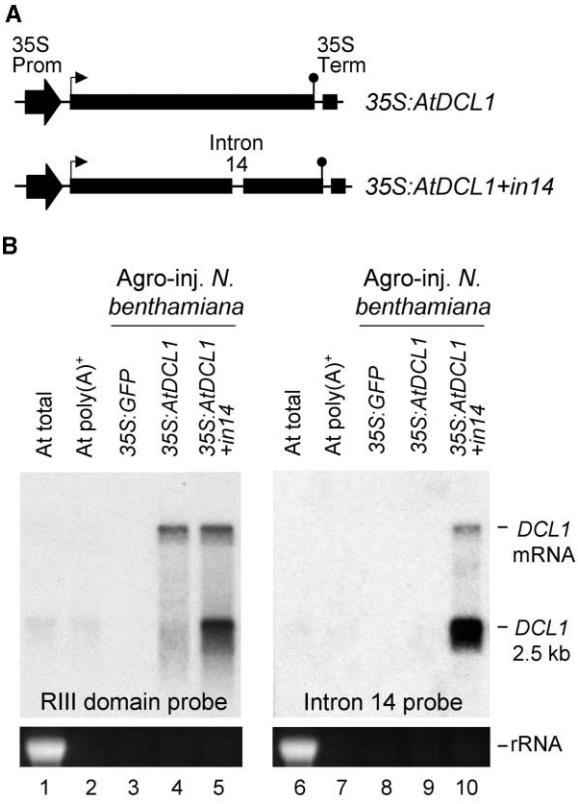

Figure 2. Effect of Intron 14 on *DCL1* RNA

(A) Diagrams of the two binary constructs used in the Agro injection assay. The *35S:AtDCL1* construct contained the 5,730 bp *DCL1* coding region and the CaMV 35S promoter and terminator sequences. The expression cassettes were cloned in pSLJ755i5. The *35S:AtDCL1+in14* construct was identical to *35S:AtDCL1*, except that the intron 14 sequence was inserted between exon 14 and exon 15.
(B) Blot hybridization of RNA from Agro-injected *Nicotiana benthamiana* leaf tissues. Constructs were Agro injected and expressed as described [16], and poly(A)$^+$-enriched RNA (0.5 μg) was extracted 2 days after injection. Controls included samples of total (25 μg) and poly(A)$^+$-enriched (0.5 μg) RNA from *Arabidopsis* and poly(A)$^+$-enriched (0.5 μg) RNA from Agro-injected *N. benthamiana* that expressed *35S:GFP*. Blots were hybridized with a radiolabeled RNase III domain probe (left panel) or an intron 14 probe (right panel). The helicase domain probe for detection of the 4.0 kb RNA was not used in these experiments because the 4.0 kb RNA is not present in poly(A)$^+$-enriched RNA fractions (see Figure 1).The ethidium bromide-stained gels in the zone corresponding to the large rRNA are also shown.

homogeneity of 3′ RACE sequences. In contrast, the 2.5 kb RNA is likely sensitive to endonucleolytic and/or exonucleolytic degradation at the 5′ end, resulting in removal of varying amounts of intron 14 (including the lariat structure) and adjoining exon sequences (Figure 1C). Intron 14 (276 bp) is approximately three times larger than the mean length of the other 18 *DCL1* introns (86.4 ± 5.4 bp), and it is possible that this sequence contributes unique functions. Interestingly, the intron 14 sequence downstream from the predicted lariat branch-junction site is predicted to form an extended fold-back structure that resembles known *Arabidopsis* miRNA precursors. Blot assays of *Arabidopsis* small RNA with radiolabeled sense and antisense probes from intron 14, however, provided no evidence for miRNAs originating from this region (data not shown).

Cleavage of *DCL1* RNA at a Predicted miRNA Interaction Site

In addition to the 5′ RACE products from the 2.5 kb RNA (Figure 1C), a larger product corresponding to an RNA species with a 5′ end from the middle of *DCL1* mRNA was identified (Figure 3A, lane 1). The 5′ end of each of 12 clones analyzed from this product mapped to the same position, one nucleotide before the exon 12/exon 13 boundary. This position corresponds to the middle of a sequence that was predicted to base-pair with miR162 (Figure 3A). miR162 was identified in two independent small RNA libraries prepared from seedling and inflorescence tissue [17] (C. Llave, K.D. Kasschau, and J.C.C., unpublished data). Cleavage of target RNA at a central site within the region of complementarity is a diagnostic feature of RISC complexes guided by both siRNA and miRNA [7, 9, 13, 18]. At least 14 *Arabidopsis* mRNAs are known to be susceptible to miRNA-guided cleavage, and each occurs opposite of the site ~10–11 positions from the ends of the respective miRNAs [7, 9, 13]. Unlike most other known or predicted miRNA-mRNA interactions in *Arabidopsis*, interaction between miR162 and *DCL1* mRNA would require a one-nucleotide bulge in the mRNA (Figure 3A). The putative miR162 interaction site spans parts of exon 12 and exon 13.

Small RNA blot assays with extracts from *Arabidopsis* (La-*er* and Col-0 ecotypes) leaf and inflorescence tissues revealed miR162, but at relatively low levels compared to several other miRNAs, such as miR171 (Figure 3B). In La-*er* plants, miR162 was detected primarily in inflorescence tissue, although, in Col-0 plants, it was detected at similar levels in both leaf and inflorescence tissue. Accumulation of the miRNA was strongly dependent on DCL1, as *dcl1* mutant plants (*dcl1-7* allele, formerly known as *sin1-1*) [19, 20] contained no detectable miR162 (Figure 3B, lanes 2 and 5). In mutant plants containing the *hen1-1* mutation [21], both miR162 and miR171 accumulated to reduced levels (Figure 3B, lanes 3 and 6); this finding suggests that these miRNAs were only partially dependent on HEN1 (At4g20910). HEN1 is a novel protein required for efficient production or activity of several miRNAs [21]. In contrast, miR162 accumulated to higher levels (3.4- to 4.9-fold) in transgenic Col-0 plants expressing a transgene encoding the *Turnip mosaic virus* (TuMV) RNA silencing suppressor, P1/HC-Pro. Comparable levels of stimulation in the presence of P1/HC-Pro were detected by using several other miRNAs in *Arabidopsis* and tobacco [13, 22]. Thus, miR162 shares several requirements and features with most other *Arabidopsis* miRNAs.

Mutations and Factors that Reduce miRNA Activity Result in Elevated *DCL1* RNA Levels

If *DCL1* mRNA is a miR162 target, then *DCL1* should be posttranscriptionally controlled by negative feedback. If DCL1 is active and miR162 is produced, then *DCL1* RNA levels should be relatively low due to miR162-guided cleavage and degradation. This model predicts that *dcl1-7* RNA encoding a debilitated protein, which

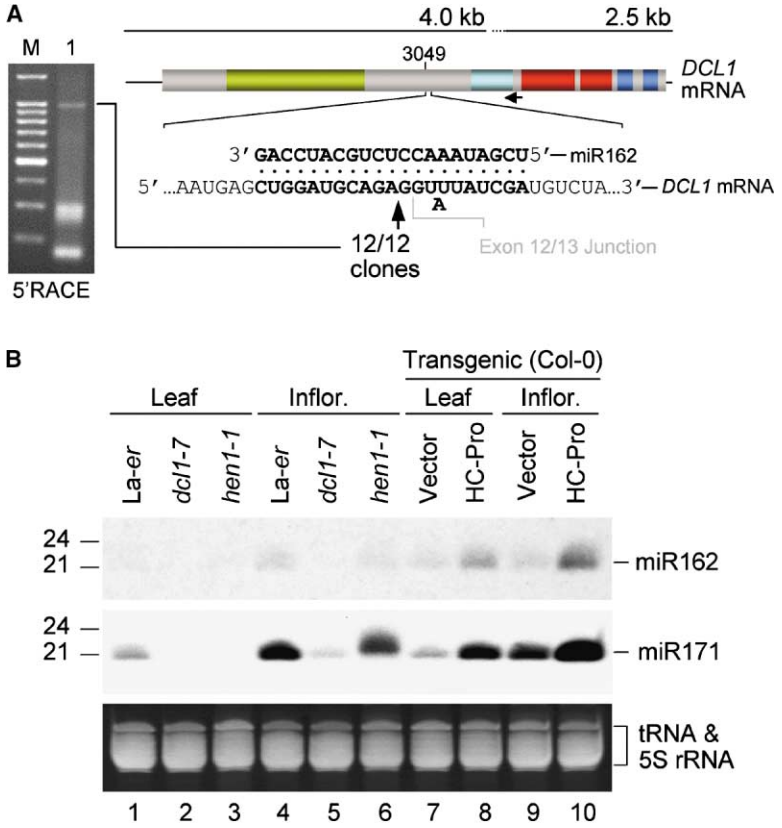

Figure 3. miR162-Guided Cleavage of *DCL1* mRNA

(A) Diagrammatic representation of the miR162-guided cleavage site in *DCL1* mRNA. The *DCL1* mRNA and 4.0 kb and 2.5 kb RNAs are shown at the top. The sequence corresponding to the miR162 interaction site in *DCL1* mRNA is shown. The position inferred as the 5′ end of a miR162-guided cleavage product, as revealed by sequence analysis of 5′ RACE products (lane 1), is indicated by the vertical arrowhead. The horizontal arrowhead indicates the location of the gene-specific 5′ RACE primer (see Figure 1C). The position of the exon 12 and exon 13 junction is also indicated.

(B) RNA blot analysis of miR162. Low-molecular weight RNA (25 μg) from leaf and inflorescence tissues of parental plants (La-*er*, lanes 1 and 4), *dcl1-7* (lanes 2 and 5), and *hen1-1* (lanes 3 and 6) mutant plants and from vector-transformed (lanes 7 and 9) and P1/HC-Pro-expressing (lanes 8 and 10) transgenic plants was prepared and analyzed as described [15]. The blot was probed with an end-labeled oligonucleotide that was complementary to miR162 (upper panel). The same filter was stripped and reprobed with a radiolabeled oligonucleotide that was complementary to miR171 (middle panel). The ethidium bromide-stained gel in the zone corresponding to tRNA and 5S RNA, prior to blot transfer, is shown (bottom panel).

results in low or limited amounts of miRNA, will accumulate to relatively high levels in mutant plants. The model also predicts that wild-type *DCL1* RNA levels will increase in plants with mutations, such as *hen1-1*, that negatively affect miRNA production or activity. Both of these predictions were tested.

RNA blot assays (RNaseIII domain probe) for *DCL1* or *dcl1-7* RNAs were done by using leaf and inflorescence tissue extracts from La-*er* control and *dcl1-7* and *hen1-1* mutant plants. *DCL1* mRNA and 2.5 kb RNA in La-*er* tissues accumulated to relatively low levels that were difficult to detect under standard hybridization condi-

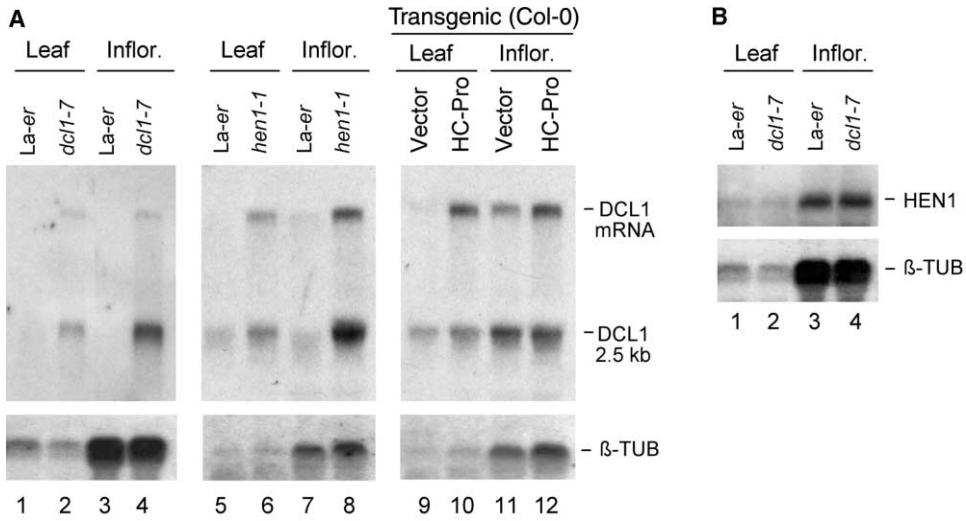

Figure 4. Effect of *dcl1-7* and *hen1-1* Mutations and TuMV P1/HC-Pro on *DCL1* mRNA Accumulation

(A) RNA blots containing poly(A)$^+$-enriched (lanes 1–4) or total RNA (lanes 5–12) were analyzed by using a radiolabeled probe corresponding to the *DCL1* RNase III domain coding sequence. Samples were from leaf or inflorescence tissue of La-*er*, *dcl1-7*, or *hen1-1* plants, as indicated above each panel. The blots were stripped and hybridized with a β-tubulin-specific probe [13] (lower panels).

(B) RNA blot assays of leaf and inflorescence tissue from La-*er* and *dcl1-7* mutant plants with a radiolabeled probe corresponding to nucleotides 2034–2677 of the *HEN1* coding sequence (upper panel). The blot was stripped and hybridized with a β-tubulin-specific probe (lower panel).

tions (Figure 4A, lanes 1, 3, 5, and 7). However, *dcl1-7* mutant mRNA accumulated in leaf and inflorescence tissue to levels that were 2.6- and 2.8-fold higher, respectively, than those in La-*er* plants (Figure 4, lanes 2 and 4). These effects were specific to the *dcl1* mRNA, as neither β-tubulin (At5g23860) nor *HEN1* mRNA was affected by the *dcl1-7* mutation (Figures 4A and 4B). In leaf and inflorescence tissue from *hen1-1* mutant plants, *DCL1* mRNA accumulated to 3.7- and 3.2-fold higher levels compared to those in La-*er* plants. Interestingly, the levels of the 2.5 kb *dcl1-7* or *DCL1* RNA in *dcl1* and *hen1* mutant plants, respectively, were elevated to amounts that were comparable to the increase of full-length mRNA (Figure 4A).

To further test the hypothesis that *DCL1* RNA is negatively regulated by miRNA-guided degradation, the effects of TuMV P1/HC-Pro on *DCL1* RNAs were tested. This RNA silencing suppressor inhibits siRNA and miRNA-guided cleavage of target RNAs [13, 16]. Leaf tissue in transgenic (Col-0) plants expressing P1/HC-Pro accumulated *DCL1* mRNA to a 4.3-fold higher level than in leaves of vector-transformed control plants (Figure 4A, lanes 9 and 10). A modest 1.7-fold increase of *DCL1* mRNA was detected in inflorescence tissues expressing P1/HC-Pro. In contrast to the mutant plants, however, little or no increase in the level of 2.5 kb *DCL1* RNA was detected in the presence of P1/HC-Pro.

These data are compatible with the *DCL1* regulatory model shown in Figure 5A. Wild-type *DCL1* mRNA is proposed to be maintained at relatively low levels because functional DCL1 protein catalyzes formation of miRNAs, at least one of which (miR162) targets *DCL1* mRNA for degradation. This end product (miRNA)-mediated inhibition would maintain DCL1 at functionally sufficient, but not limiting or excessive, levels. Elevated levels of DCL1 would trigger more rapid or prolonged periods of degradation of *DCL1* pre-mRNA and mRNA, whereas limiting levels of DCL1 would lead to derepression and new protein production. miRNA-deficient *dcl1* plants lack sufficient miR162 and, therefore, accumulate high levels of *dcl1* mRNA (Figure 5B). Similarly, miRNA-suppressed *hen1* plants have defects in miRNA biosynthesis or activity, resulting in derepression of *DCL1*. TuMV P1/HC-Pro derepresses *DCL1* by suppression of miRNA-guided cleavage activity, not through inhibition of miRNA generation (Figure 5C) [13]. This may also explain why miRNAs accumulate to higher levels in the presence of P1/HC-Pro. Increased levels of *DCL1* mRNA may lead to higher levels of DCL1 protein, which may increase the capacity for miRNA precursor processing.

The response of full-length and truncated forms of *DCL1* RNAs in the different genetic backgrounds may be informative about the site of miRNA activity. Because both full-length mRNA and 2.5 kb truncated RNAs are sensitive to active DCL1 and HEN1 (Figure 4, lanes 1–8), and because the miR162 interaction site is not present in the 2.5 kb RNA, we propose that miR162-guided cleavage occurs on partially spliced pre-mRNA in the nucleus. It is also likely that *DCL1* mRNA is sensitive to cleavage in the cytoplasm, as the mRNA accumulates to elevated levels in the presence of P1/HC-Pro. The HC-Pro protein encoded by closely related viruses, such as *Cowpea aphid-borne mosaic virus* [23] and *Tobacco etch virus* (unpublished data), was shown to accumulate in the cytoplasm. DCL1 is predicted to contain a nuclear targeting signal [14], although DCL1 localization data are presently lacking. It is also possible that there are additional miRNA target sites or DCL1-sensitive processing sites in the 2.5 kb RNA.

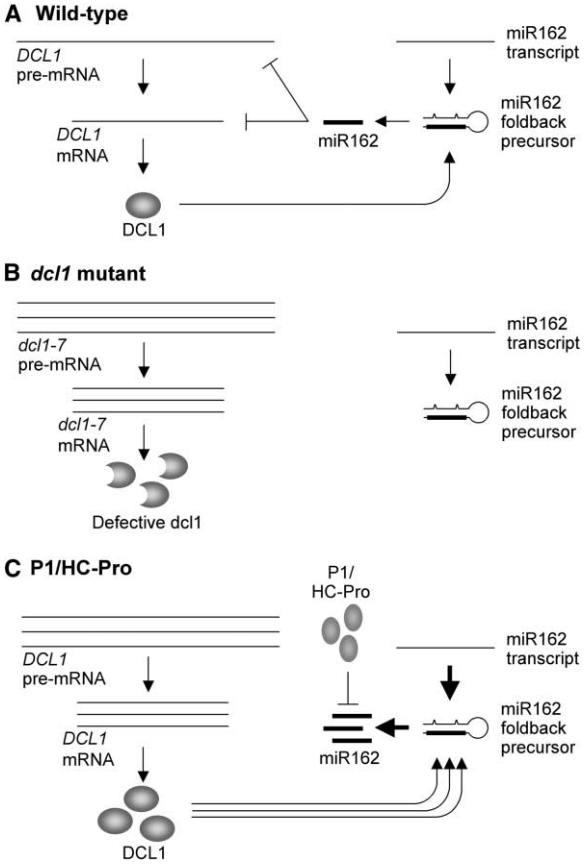

Figure 5. Model of Negative Feedback Regulation of *DCL1* in *Arabidopsis*

(A) In wild-type *Arabidopsis*, *DCL1* mRNA is maintained at a low level due to miR162-directed cleavage and subsequent degradation.
(B) In the *dcl1* mutant, defective dcl1 protein results in a deficiency of miR162. *DCL1* RNA accumulates to higher levels due to a lack of miR162-guided cleavage.
(C) In TuMV P1/HC-Pro-expressing transgenic plants, *DCL1* mRNA accumulates to a higher level due to suppression of miR162-guided cleavage. miR162 (and other miRNAs) accumulates to higher levels because elevated levels of DCL1 may drive miR162 precursor processing.

Finally, although there is no established connection between the intron 14-associated aberrant splicing of *DCL1* pre-mRNA and the miRNA-mediated regulation of *DCL1*, the possible role of intron 14 in *DCL1* expression is rather intriguing. Further study is required to test whether the relatively stable 4.0 kb and 2.5 kb *DCL1* RNA species serve any biological function.

Acknowledgments

We thank Dr. Xuemei Chen (Rutgers University) for providing *hen1-1* seeds. We also thank Lisa Johansen and Cesar Llave for valuable discussions during this study. This work was supported by grants

from the National Science Foundation (MCB-0209836), the National Institutes of Health (AI43288), and the U.S. Department of Agriculture (NRI2002-35319-11560).

Received: February 27, 2003
Revised: March 14, 2003
Accepted: March 14, 2003
Published: April 29, 2003

References

1. Hannon, G.J. (2002). RNA interference. Nature *418*, 244–251.
2. Schauer, S.E., Jacobsen, S.E., Meinke, D.W., and Ray, A. (2002). *DICER-LIKE1*: blind men and elephants in *Arabidopsis* development. Trends Plant Sci. *7*, 487–491.
3. Bernstein, E., Caudy, A.A., Hammond, S.M., and Hannon, G.J. (2001). Role for a bidentate ribonuclease in the initiation step of RNA interference. Nature *409*, 363–366.
4. Finnegan, E.J., Margis, R., and Waterhouse, P.M. (2003). Post-transcriptional gene silencing is not compromised in the *Arabidopsis* CARPEL FACTORY (DICER-LIKE1) mutant, a homolog of Dicer-1 from *Drosophila*. Curr. Biol. *13*, 236–240.
5. Pasquinelli, A.E., and Ruvkun, G. (2002). Control of developmental timing by microRNAs and their targets. Annu. Rev. Cell Dev. Biol. *18*, 495–513.
6. Hutvágner, G., and Zamore, P.D. (2002). A microRNA in a multiple-turnover RNAi enzyme complex. Science *297*, 2056–2059.
7. Tang, G., Reinhart, B.J., Bartel, D.P., and Zamore, P.D. (2003). A biochemical framework for RNA silencing in plants. Genes Dev. *17*, 49–63.
8. Mourelatos, Z., Dostie, J., Paushkin, S., Sharma, A., Carroux, B., Abel, L., Rappsilber, J., Mann, M., and Dreyfuss, G. (2002). miRNPs: a novel class of ribonucleoproteins containing numerous microRNAs. Genes Dev. *16*, 720–728.
9. Llave, C., Xie, Z., Kasschau, K.D., and Carrington, J.C. (2002). Cleavage of *Scarecrow-like* mRNA targets is directed by a class of *Arabidopsis* miRNA. Science *297*, 2053–2056.
10. Olsen, P.H., and Ambros, V. (1999). The lin-4 regulatory RNA controls developmental timing in *Caenorhabditis elegans* by blocking LIN-14 protein synthesis after the initiation of translation. Dev. Biol. *216*, 671–680.
11. Wightman, B., Ha, I., and Ruvkun, G. (1993). Posttranscriptional regulation of the heterochronic gene lin-14 by lin-4 mediates temporal pattern formation in *C. elegans*. Cell *75*, 855–862.
12. Rhoades, M.W., Reinhart, B.J., Lim, L.P., Burge, C.B., Bartel, B., and Bartel, D.P. (2002). Prediction of plant microRNA targets. Cell *110*, 513–520.
13. Kasschau, K.D., Xie, Z., Allen, E., Llave, C., Chapman, E.J., Krizan, K.A., and Carrington, J.C. (2003). P1/HC-Pro, a viral suppressor of RNA silencing, interferes with *Arabidopsis* development and miRNA function. Dev. Cell *4*, 205–217.
14. Jacobsen, S.E., Running, M.P., and Meyerowitz, E.M. (1999). Disruption of an RNA helicase/RNAse III gene in *Arabidopsis* causes unregulated cell division in floral meristems. Development *126*, 5231–5243.
15. Llave, C., Kasschau, K.D., Rector, M.A., and Carrington, J.C. (2002). Endogenous and silencing-associated small RNAs in plants. Plant Cell *14*, 1605–1619.
16. Johansen, L.K., and Carrington, J.C. (2001). Silencing on the spot: induction and suppression of RNA silencing in the Agrobacterium-mediated transient expression system. Plant Physiol. *126*, 930–938.
17. Reinhart, B.J., Weinstein, E.G., Rhoades, M.W., Bartel, B., and Bartel, D.P. (2002). MicroRNAs in plants. Genes Dev. *16*, 1616–1626.
18. Elbashir, S.M., Lendeckel, W., and Tuschl, T. (2001). RNA interference is mediated by 21- and 22-nucleotide RNAs. Genes Dev. *15*, 188–200.
19. Robinson-Beers, K., Pruitt, R.E., and Gasser, C.S. (1992). Ovule development in wild-type *Arabidopsis* and two female sterile mutants. Plant Cell *4*, 1237–1250.
20. Lang, J.D., Ray, S., and Ray, A. (1994). *sin1*, a mutation affecting female fertility in *Arabidopsis*, interacts with *mod1*, its recessive modifier. Genetics *137*, 1101–1110.
21. Park, W., Li, J., Song, R., Messing, J., and Chen, X. (2002). CARPEL FACTORY, a Dicer homolog, and HEN1, a novel protein, act in microRNA metabolism in *Arabidopsis thaliana*. Curr. Biol. *12*, 1484–1495.
22. Mallory, A.C., Reinhart, B.J., Bartel, D., Vance, V.B., and Bowman, L.H. (2002). A viral suppressor of RNA silencing differentially regulates the accumulation of short interfering RNAs and micro-RNAs in tobacco. Proc. Natl. Acad. Sci. USA *99*, 15228–15233.
23. Mlotshwa, S., Verver, J., Sithole-Niang, I., Gopinath, K., Carette, J., Vankammen, A., and Wellink, J. (2002). Subcellular location of the helper component-proteinase of Cowpea aphid-borne mosaic virus. Virus Genes *25*, 207–216.